

# A CONSISTENT PIXEL-WISE BLUR MEASURE FOR PARTIALLY BLURRED IMAGES

Xianyong Fang<sup>†‡</sup>, Feng Shen<sup>†</sup>, Yanwen Guo<sup>‡</sup>, Christian Jacquemin<sup>\*</sup>, Jian Zhou<sup>†</sup>, Shanchun Huang<sup>†</sup>

<sup>†</sup> Key Lab. of Intelligent Computing and Signal Processing, Anhui University, Hefei, 230601, China

<sup>‡</sup>State Key Lab. for Novel Software Technology, Nanjing University, Nanjing, 210023, China

<sup>\*</sup>AMI, LIMSI-CNRS, Orsay, 91403, France

## ABSTRACT

Despite numerous efforts on blur measurement of partially blurred images, there still lacks an effective blur measure that is both pixel-wise and locally sharp consistent. The paper proposes a novel method with two contributions to overcome this limitation: 1) A new pixel-based blur metric, Multi-resolution Singular Value (MSV), which leverages the average singular value of high frequency bands to measure the blur of each pixel, and 2) a locally continuous strategy, maximum-likelihood estimation (MLE) based refinement, that ensures local continuity by imposing the local sharp consistency on pixel blur in a local correcting process. Experimental results show that our method is effective to smoothly measure the partially blurred images without local discontinuity.

**Index Terms**— Blur metric, singular value, maximum-likelihood estimation

## 1. INTRODUCTION

Partially blurred images are very common in our daily photographing. Obtaining the blur degree of each pixel is important for further processing, such as segmentation, image fusion and deblurring. However, there still lacks an effective blur measurement method which measures the image in a pixel-wise and locally sharp consistent manner. In this paper, we propose a simple yet robust method aiming for efficient pixel-wise blur measurement.

Edge is widely used due to its representation of high frequency information. Existing edge-based methods [1, 2, 3, 4, 5, 6, 7, 8]) may not be good for detecting the locally blurred area where only sparse edges exist. Non edge-based methods for the global blur evaluation of a whole image [9, 10, 11, 12, 13] may also be invalid due to the insufficient information in a locally blurred area. Methods work on patch or block [14, 15, 16, 17]) are rough, thus easily leading to false evaluation of each pixel and zigzagged edges of the blurred area. Therefore, we prefer to the pixel-wise blur metric using non-edge based method for a smooth measurement.

We are interested in the simple metric proposed by Bolan Su *et al.* [18]. The ratio of the largest several singular values to all singular values is taken as the blur metric. It will

be higher for a blurred image than a clear image because the largest singular values represent the large scales. While other methods [19, 20] heavily rely on specific image blurring models for computing the defocusing blur or linear motion blur, this metric works for any type of blur. Terming it as Direct Ratio (DR), however, we argue that its mandatory usage of the singular values from the whole image frequency range can be unstable, considering the fact that blur influences the high frequency bands much more than the low frequency part.

In addition, most existing methods [18, 21, 3, 20] do not consider refining the local blur measurement after obtaining the blur measurement of each pixel or block. However, noise or other metric-resistance factors may affect the local blur measurement and lead to measurement errors. Although Zhu *et al.* [19] considered generating a coherent blur map by assuming the scale consistency, they relied on the global energy minimization method  $\alpha$ -cut [22] which is sensitive to initialization.

We propose a new blur measurement method that measures blur in a pixel-wise and locally sharp consistent way. For the pixel-wise measurement, a new blur metric, Multi-resolution Singular Value (MSV), is introduced. Unlike DR of Bolan Su *et al.* [18], MSV drops the less affected low frequency band and only uses the average value of the high frequency bands obtained from the multi-resolution decomposition by Haar wavelet transform of the block surrounding each pixel. To achieve local consistent measurement, a refinement strategy based on maximum-likelihood estimation (MLE) is introduced to improve the initial result of MSV. In comparison with the scale consistency assumption of Zhu *et al.* [19], our MLE based refinement is more simple, robust and easy to apply.

## 2. THE MSV BLUR METRIC

An image  $I$  can be decomposed into weighted sum of  $n$  eigenimages by Singular Value Decomposition (SVD),

$$I = \sum_{i=1}^n \lambda_i E_i \quad (1)$$

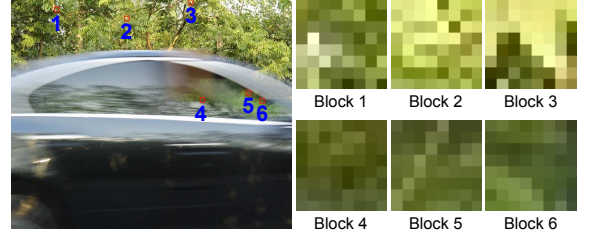
where  $\lambda_i (1 \leq i \leq n)$  are the eigen values in decreasing order and  $\mathbf{E}_i (1 \leq i \leq n)$  are rank-1 matrices called eigen-images. The first most significant eigen-images work on large scales while less significant eigen-images encode the image details. For a blurred block, the high frequency details are lost much more significantly in comparison with its low frequency shape structures. Therefore, we drop the contribution coming from the low frequency information and only consider the eigen values from the high frequency structures. In particular, we use the average eigen value of high frequency bands of the block surrounding each pixel as the blur metric of that pixel, where the bands are generated by the multi-resolution decomposition of the Haar wavelet transform. We call this metric Multi-resolution Singular Value (MSV).

Fig. 1 shows a partially blurred image with six  $8 \times 8$  blocks extracted for comparison between MSV and DR which considers the blur response from both low frequency structures and high frequency details. One half of the blocks are clear, while the other half are blurred. Each block is decomposed by the Haar wavelet transform into four bands LL, LH, HH and HL. They represent the horizontal low-pass/vertical low-pass (LL), horizontal low-pass/vertical high-pass (LH), horizontal high-pass/vertical high-pass (HH), and horizontal high-pass/vertical low-pass (HL), separately. For DR, it takes the ratio of the four largest singular values to all singular values as Su *et al.* [18] have done. As shown in Fig. 1(b), the ratios of the clear blocks by DR, which should be higher than those of the blurred blocks, are even all slightly lower than them. But the average eigen value of either each highest frequency band (LH, HH and HL) or all of them from the clear blocks is significantly greater than those from the blurred blocks. This figure clearly shows that MSV can measure the blur extent of each pixel robustly and DR, however, may fail due to the affection of the lower frequency structures.

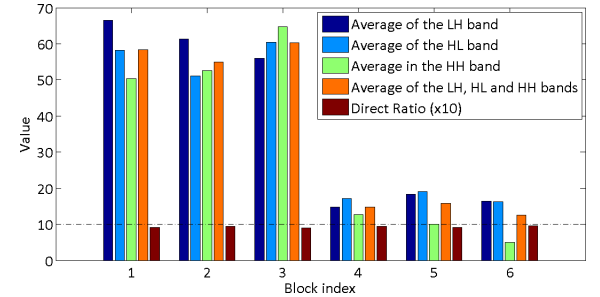
As shown in Fig. 2, the MSV metric of a pixel is computed with the  $m \times m$  block surrounding it. Denote the singular values from LH, HL and HH of the block as  $\mathbf{T}_1$ ,  $\mathbf{T}_2$  and  $\mathbf{T}_3$  respectively, with  $\mathbf{T}_i = (\lambda_{i_1}, \lambda_{i_2}, \dots, \lambda_{i_{m/2}})$  for  $1 \leq i \leq 3$  and  $\lambda_{i_k} (1 \leq k \leq m/2)$  being the eigen values in decreasing order. The MSV metric is computed as the weighted average of the means of  $\mathbf{T}_i$ ,  $\bar{\mathbf{T}}_i$ ,

$$S = \sum_{i=1}^3 w_i \bar{\mathbf{T}}_i. \quad (2)$$

The weights  $w_i$  of Equation 2 balance the influences of each high frequency band. They are set experimentally considering the efficient combination of the three high frequency bands. All the three bands contribute nearly equally to the blur appearance in our experiments. Therefore, in practice, we set  $w_1 = w_2 = w_3 = 1/3$ . That is, they are equally weighted.



(a) The partially blurred image and six extracted blocks shown on the right for a clear view.



(b) Comparison of the average singular values of each high frequency band and all high frequency bands with the ratio by DR.

**Fig. 1.** Comparison of MSV with DR by six  $8 \times 8$  blocks indexed from 1 to 6 with half of them blurred. LH, LH and HH are the high frequency bands used in MSV. Note: the ratios of DR are scaled by 10 for a clear view.

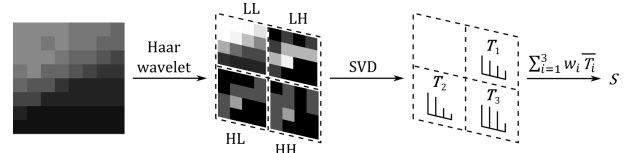


**Fig. 2.** The computation of the MSV metric for a pixel by its surrounding  $m \times m$  block.  $\mathbf{T}_i$  represents the vector form of the singular values of the corresponding band image.

### 3. MLE BASED REFINEMENT

The pixel-wise MSV blur metric omits the contribution from the surrounding pixel and may lead to false measure due to noise and local structure variations. Here we introduce a refinement strategy based on MLE to improve the result of MSV.

Denote the blur measure of a pixel  $I_c$  and all  $l$  pixels  $I_j (1 \leq j \leq l)$  in its surrounding region  $\Omega$  as  $S_c$  and  $S_j (1 \leq j \leq l)$ , respectively. Motivated by the consistency of blur in a local area,  $S_j (1 \leq j \leq l)$  can be considered i.i.d. random observations, coming from a distribution  $p(\cdot | S_c)$ . The blur likelihood of  $S_c$  can be formulated as

$$\mathcal{L}(S_c | S_1, S_2, \dots, S_l) = \prod_{j=1}^l p(S_j | S_c) \quad (3)$$

which can be rewritten into the following log-likelihood

$$\ln \mathcal{L}(S_c | S_1, S_2, \dots, S_l) = \sum_{j=1}^l \ln p(S_j | S_c). \quad (4)$$

The straightforward way to find the optimal blur measure of pixel  $I_c$ ,  $\hat{S}_c$ , is to maximize the log-likelihood of Equation 4, *i.e.*,

$$\hat{S}_c = \arg \max_{S_c} \ln \mathcal{L}(S_c | S_1, S_2, \dots, S_l) \quad (5)$$

which can be solved by the likelihood equation

$$\frac{\partial \ln \mathcal{L}(S_c | S_1, S_2, \dots, S_l)}{\partial S_c} = 0. \quad (6)$$

The closer  $I_j$  is to  $I_c$ , the closer  $S_j$  is to  $S_c$ . Therefore, in our current implementation, Gaussian distribution is adopted to model such a conditional distribution, *i.e.*,

$$p_j(S_j | S_c) \propto \frac{1}{2\pi} \exp\left[-\frac{(S_j - S_c)^2}{2\sigma^2}\right] \quad (7)$$

where  $\exp$  represents the exponential function with  $\sigma$  set to be 1 in our experiment. Taking Equation 7 into Equation 6, we finally obtain

$$\hat{S}_c = \frac{\sum_{j=1}^l S_j}{l} \quad (8)$$

which is the average blur measure of the surrounding pixels.

### 3.1. The blur measurement algorithm

Directly applying the MLE-based refinement to all pixels might lead to over blurred or clear pixels. Instead, we only apply it to the incorrectly measured pixels. A binary blur property  $B_c$  is used to label  $I_c$  as blurred or clear by checking whether  $S_c$  is smaller than the threshold  $\epsilon_t$  or not.  $I_c$  is incorrectly measured when  $B_c$  is not the same as the labels of most of its surrounding pixels. We propose to recursively update the incorrect measures with two passes, as presented in Algorithm 1. Steps 4 – 7 represent the blur pass for eliminating the falsely measured blurred pixels and steps 8 – 11 denote the clear pass for eliminating falsely measured clear pixels.

In practice, we set the block size to  $11 \times 11$ .  $\epsilon_t$  affects the results of Algorithm 1 and normally  $\epsilon_t = 32$ . Whether a pixel is falsely labeled or not depends on the number of differently labeled surrounding pixels, which we set it to 90, and it works well with our experiment.

## 4. EXPERIMENTAL RESULTS

We verify the effectiveness of our method by experimenting with a variety of images, and compare with the DR metric [18] which represents state-of-the-art blur measure methods. Fig. 3 gives the blur measurement for the image shown in Fig.

---

**Algorithm 1** Blur measurement by MSV and MLE based refinement

---

**Input:** An image,  $I$

**Output:** Matrices  $M$  and  $B$  recording the blur measures and properties of all pixels in  $I$  respectively

```

1: Initialize  $M$  (Equation 2);
2: Initialize  $B$ ;
3: repeat
4:   while exist a pixel falsely labeled as blur in  $B$  do
5:     Update its blur measure in  $M$  (Equation 5);
6:     Update its label in  $B$ ;
7:   end while
8:   while exist pixel falsely labeled as clear in  $B$  do
9:     Update its blur measure in  $M$  (Equation 5);
10:    Update its label in  $B$ ;
11:  end while
12: until no wrong measure or reaching the max iterations

```

---

1(a). The six central pixels shown in Fig. 1(a) are detected by MSV (Figure 3(b)) while DR fails to correctly return their measures (Fig. 3(a)). However, as shown progressively in Fig. 3(c) and Fig. 3(d), the proposed method can obtain a more smooth measurement than DR by applying the MLE based refinement strategy.

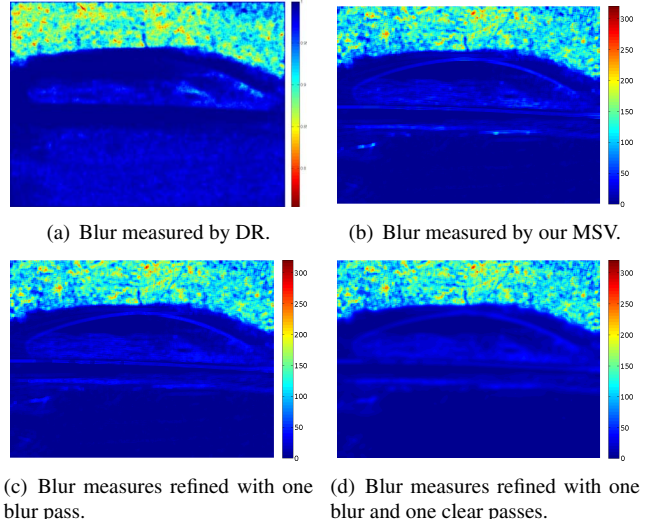


**Fig. 3.** Comparison of blur measures between DR and MSV for the image shown in Fig. 1(a).

Fig. 4 shows the labeling result for the image shown in Fig. 1(a). Fig. 4(a) is the best result for Fig. 3(a). Apparently there are some misclassifications due to the false measures. However, the blur region according to the labels by our method (Fig. 3(d)) returns no visible artifacts.

Fig. 5 shows the results on four images. DR fails to obtain a locally sharp consistent measurement for each image while our method yields locally consistent results for all of them



(a) The blurred region for Fig. 3(a). (b) The blurred region for Fig. 3(d).

**Fig. 4.** Comparison of the blurred regions according to the labels obtained by DR and our method for the image shown in Fig. 1(a). The pixels whose blur properties are blurred are whitened with the clear ones kept the same as their original pixel intensities for a clear view.

due to the benefits of the proposed refinement strategy.

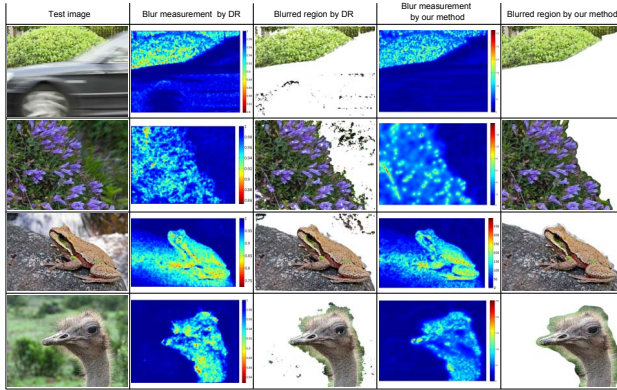


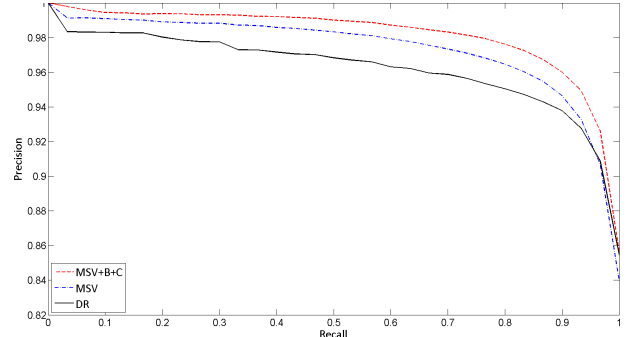
**Fig. 5.** More comparisons between DR and our method. The blurred region is the labeling result shown in the same way as Fig. 4.

We also compare the statistical performance of DR and our method with 50 partially blurred images using the precision-recall curve. They are blurred by motion or defocusing. Each image is manually segmented into a blurred region and a clear region as the ground truth label for each pixel. The threshold of DR for labeling ranges from 0 to 0.5 while the threshold of our method ranges from 0 to 1 by normalizing the blur measures of each image. In order to show the advantages of the proposed refinement strategy, we collect the precision-recall curves for MSV both without and with the refinement processing. For the refinement, one blur pass and one clear pass are applied after applying MSV and thus we denote the curve as MSV+B+C. Fig. 6 gives the comparison result along with some test images and their ground-truth labels obtained manually (Fig. 6(a)). The precision of MSV is almost always better than DR when recall is less than 0.9, while MSV+B+C almost always obtains the highest precisions than both DR and MSV. This comparison statistically shows the advantages of the MSV blue metric

and MLE based refinement strategy.



(a) Some test images and their ground truths. The ground truths are shown in the same way as Fig. 4.



(b) The precision-recall curves.

**Fig. 6.** Statistical comparison between DR and our method.

## 5. CONCLUSIONS

This paper discusses the accurate blur measurement for the partially blurred images and proposes a method to simultaneously reach pixel-wise and locally sharp consistent blur measures. The method includes a new blur metric, MSV, to obtain initial high-quality pixel-based blur measures with the high frequency bands, and an MLE based refinement strategy to recursively obtain a locally sharp consistent measurement. The experimental results demonstrate the advantage of the proposed method.

Our method may fail for a textureless area where the singular values are generally very low. In this case, the clear area and blurred area are difficult to distinguish. The DCT-based method is reported to be efficient for such a textureless area [14] and we plan to incorporate it into our framework in the future.

## Acknowledgment

This work is co-supported by Nature Science Foundation of China (61373059, 61301295, 61300169), Anhui Provincial Nature Science Foundation (1308085QF100, 1408085MF113) and Open Foundation of the State Key Lab. for Novel Software Technology (KFT2013B12).

## 6. REFERENCES

- [1] Jorge Caviedes and Sabri Gurbuz, “No-reference sharpness metric based on local edge kurtosis,” in *ICIP*, 2002, vol. 3, pp. III–53–III–56 vol.3.
- [2] Pina Marziliano, Frederic Dufaux, Stefan Winkler, and Touradj Ebrahimi, “A no-reference perceptual blur metric,” in *ICIP*, 2002, vol. 3, pp. III–57–III–60 vol.3.
- [3] Ayan Chakrabarti, Todd Zickler, and William T Freeman, “Analyzing spatially-varying blur,” in *CVPR*, 2010, pp. 2512–2519.
- [4] Rony Ferzli and Lina J. Karam, “A no-reference objective image sharpness metric based on the notion of just noticeable blur (jnb),” *IEEE Transactions on Image Processing*, vol. 18, no. 4, pp. 717–728, 2009.
- [5] Lina J. Karam, Touradj Ebrahimi, Sheila S. Hemami, Thrasyvoulos N. Pappas, Robert J. Safranek, Zhou Wang, and Andrew B. Watson, “Introduction to the issue on visual media quality assessment,” *IEEE Journal of Selected Topics in Signal Processing*, vol. 3, no. 2, pp. 189–192, 2009.
- [6] Niranjan D. Narvekar and Lina J. Karam, “A no-reference image blur metric based on the cumulative probability of blur detection (cpbd),” *IEEE Transactions on Image Processing*, vol. 20, no. 9, pp. 2678–2683, 2011.
- [7] Hanghang Tong, Mingjing Li, HongJiang Zhang, and Changshui Zhang, “Blur detection for digital images using wavelet transform.,” in *ICME*, 2004, pp. 17–20.
- [8] Seyfollah Soleimani, Filip Rooms, and Wilfried Philips, “Efficient blur estimation using multi-scale quadrature filters,” *Signal Processing*, vol. 93, no. 7, pp. 1988 – 2002, 2013.
- [9] Xavier Marichal, Wei-Ying Ma, and HongJiang Zhang, “Blur determination in the compressed domain using DCT information,” in *ICIP*, 1999, vol. 2, pp. 386–390.
- [10] Ming-Jun Chen and Alan C. Bovik, “No-reference image blur assessment using multiscale gradient,” *EURASIP Journal on Image and Video Processing*, vol. 2011, pp. 1–11, 2011.
- [11] Doron Shaked and Ingeborg Tastl, “Sharpness measure: towards automatic image enhancement,” in *ICIP*, 2005, vol. 1, pp. I–937–40.
- [12] Matej Kristan, Janez Perš, Matej Perše, and Stanislav Kovačič, “A bayes-spectral-entropy-based measure of camera focus using a discrete cosine transform,” *Pattern Recognition Letters*, vol. 27, no. 13, pp. 1431–1439, 2006.
- [13] Rania Hassen, Zhou Wang, and Magdy Salama, “No-reference image sharpness assessment based on local phase coherence measurement,” in *ICASSP*, 2010, pp. 2434–2437.
- [14] Erik Kalalembang, Korendianto Usman, and Irwan Prasetya Gunawan, “DCT-based local motion blur detection,” in *ICICI-BME*, 2009, pp. 1–6.
- [15] V. Kanchev, K. Tonchev, and Ognian Boumbarov, “Blurred image regions detection using wavelet-based histograms and SVM,” in *IDAACS*, 2011, pp. 457–461.
- [16] Renting Liu, Zhaorong Li, and Jiaya Jia, “Image partial blur detection and classification.,” in *CVPR*. 2008, pp. 1–8, IEEE Computer Society.
- [17] Phong V. Vu and Damon M. Chandler, “A fast wavelet-based algorithm for global and local image sharpness estimation,” *IEEE Signal Processing Letters*, vol. 19, no. 7, pp. 423–426, 2012.
- [18] Bolan Su, Shijian Lu, and Chew Lim Tan, “Blurred image region detection and classification,” in *ACM Multimedia*, 2011, pp. 1397–1400.
- [19] Xiang Zhu, Scott Cohen, Stephen Schiller, and Peyman Milanfar, “Estimating spatially varying defocus blur from a single image,” *IEEE Transactions on Image Processing*, vol. 22, no. 12, pp. 4879–4891, 2013.
- [20] Florent Couzinié-Devy, Jian Sun, Kartek Alahari, Jean Ponce, et al., “Learning to estimate and remove non-uniform image blur,” in *CVPR*, 2013, pp. 1075–1082.
- [21] Anat Levin, “Blind motion deblurring using image statistics,” in *Advances in Neural Information Processing Systems 19*, B. Schölkopf, J. Platt, and T. Hoffman, Eds., pp. 841–848. MIT Press, 2007.
- [22] Yuri Boykov, Olga Veksler, and Ramin Zabih, “Fast approximate energy minimization via graph cuts,” *IEEE Transactions on Pattern Analysis and Machine Intelligence*, vol. 23, no. 11, pp. 1222–1239, 2001.